Electronic Supplementary Material (ESI) for Energy Advances.

Supporting Documents

Synergistic photo enhanced electrocatalysis of Pt-ZnO-Bi_2O_3 heterojunction for methanol oxidation under visible light illumination

Kamal Kanti Bera[a], Malay Chakraborty[a], Shyamal Kanti Bera[b], Anupam Chowdhury[a], Mahima Ranjan Das[c], Mousumi Mondal[a], ***Swapan Kumar Bhattacharya[a]****

[a]*Physical Chemistry Section, Department of Chemistry, Jadavpur University, Kolkata – 700032, India.

[b]School of Chemical Science, National Institute of Science Education and Research (NISER) Bhubaneswar -752050, India

[c]Department of Physics, The University of Burdwan, Burdwan – 713104, India.

*Email – swapankumarbhattacharya@gmail.com

Tel. : 919831699643, Fax: +91332414

Table S1. Composition from Rietveld analysis and average particle size of Pt in different binary and ternary synthesized composite from TEM analysis.

Sample Name	Mass% from experimental	Mass% from Reitveld analysis	R_{wp}	R_{exp}	GoF	Latice parameter in A						Average particle diameter of Pt from TEM (nm)	Microstrain
						Pt	ZnO		Bi_2O_3				
						a	a	c	a	b	c		
Pt XC72	Pt- 10 C-90	Pt-10.64 C- 89.36	13.25	11.76	1.12	3.89						1.81±1.90	0.00986
Pt-Bi_2O3 (PB)	Pt-23.60 Bi_2O_3-76.4	Pt-25.68 Bi_2O_3-74.32	12.24	11.13	1.09	3.89			5.842	8.152	7.485	3.51±0.27	0.00052
Pt-ZnO (PZ)	Pt-23.6 ZnO-76.4	Pt-21.44 ZnO-98.56	9.65	8.92	1.08	3.90	3.240	5.211				2.13±0.41	0.00056
PZ1B5	Pt-23.6 Bi_2O_3-71.37 ZnO -5.03	Pt-21.78 Bi_2O_3-72.13 ZnO - 6.09	11.23	10.57	1.06	3.90	3.245	5.210	5.842	8.146	7.498	4.35±0.70	0.00126
PZ1B1	Pt-23.6 ZnO-56.63 ZnO-19.77	Pt-20.23 Bi_2O_3-61.12 ZnO-18.65	13.23	11.85	1.12	3.88	3.240	5.209	5.846	8.147	7.492	3.36±0.34	0.00178
PZ5B1	Pt-23.6 Bi_2O_3-27.85 ZnO -48.55	Pt-21.13 Bi_2O_3-25.76 ZnO - 49.11	9.654	8.92	1.08	3.88	3.246	5.211	5.843	8.157	7.516	2.84±0.30	0.00165
PZ20B1	Pt-23.6 Bi_2O_3-9.57 ZnO -66.82	Pt-21.98 Bi_2O_3-10.67 ZnO-67.35	14.23	12.92	1.10	3.90	3.249	5.217	5.856	8.155	7.512	2.77±1.1	0.00068
PZ25B1	Pt-23.6 Bi_2O_3-7.82 ZnO -68.58	Pt-21.54 Bi_2O_3-8.92 ZnO - 69.54	9.87	8.74	1.12	3.89	3.248	5.218	5.853	8.148	7.514	2.51±0.44	0.00094
PZ30B1	Pt-23.6 Bi_2O_3- 6.83 ZnO-69.46	Pt-24.2 Bi_2O_3 7.10 ZnO - 68.68	10.24	8.98	1.14	3.89	3.246	5.215	5.846	8.152	7.503	3.10±0.62	0.00075

Fig. S1 Rietveld investigation output of PXRD of as-prepared nanocatalysts. The observed (I_0) and calculated (I_c) intensity of XRD patterns are indicated in black and red solid lines respectively. Here, I_0-I_c stands for the residual intensity.

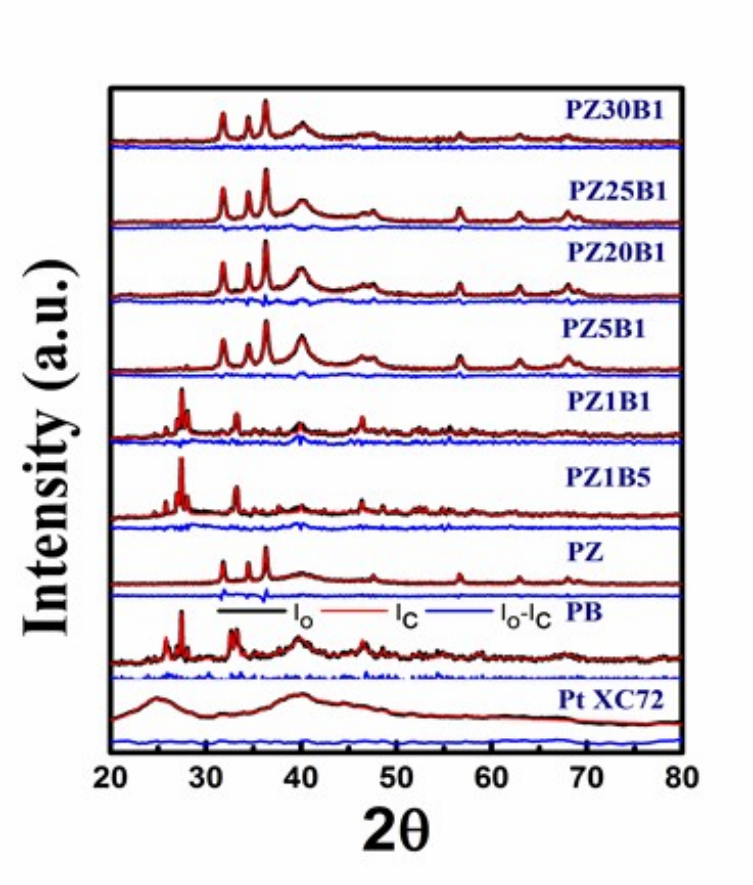

Fig. S2 TEM images (a) PtXC72 (b) PZ1B5 (c) PZ1B1 (d) PZ5B1 (e) PZ20B1 (f) PZ30B1. Inset of each figure (Histogram) represents corresponding particle size distribution of Pt.

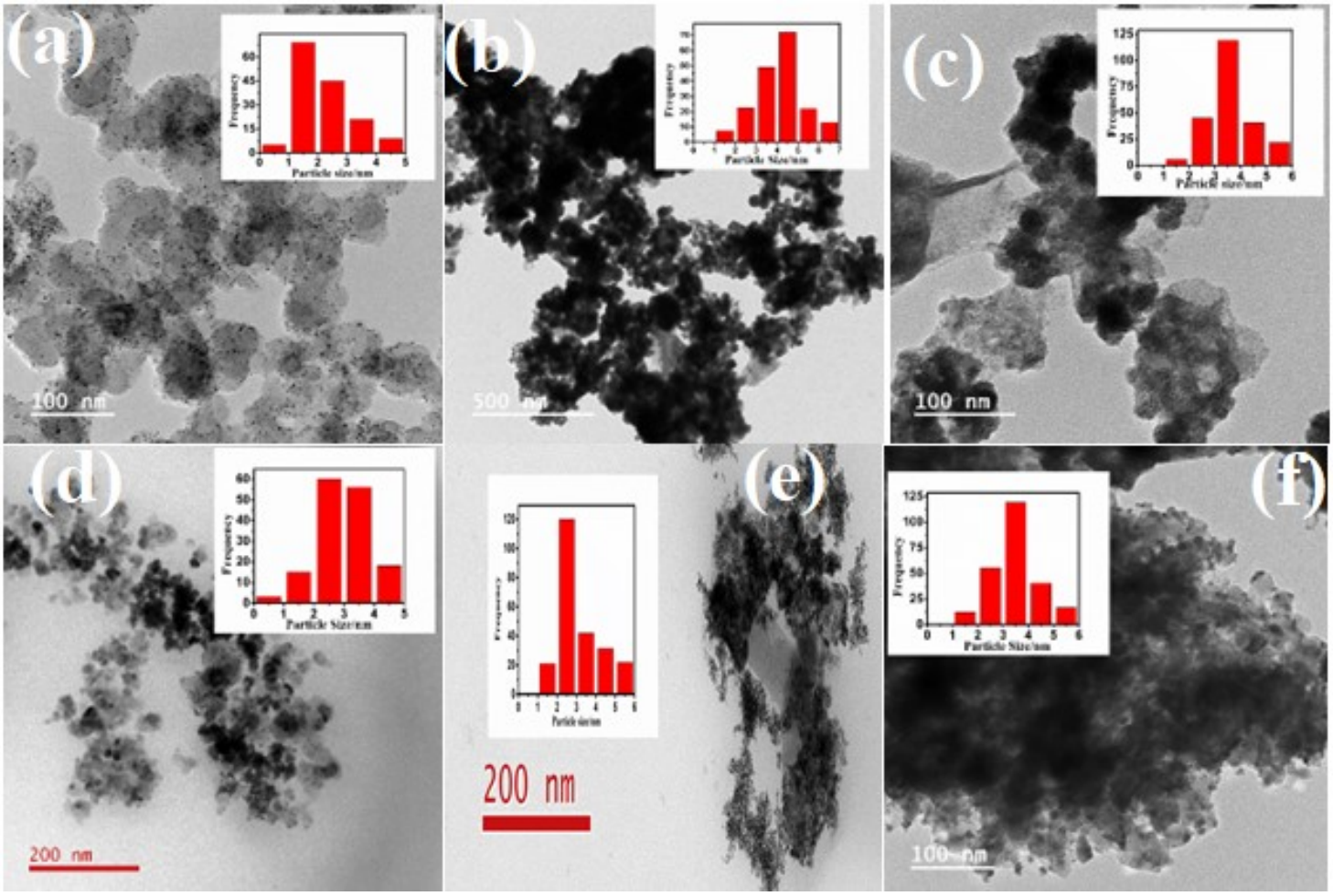

Fig. S3 XPS profile of Pt-Bi_2O_3(PB)

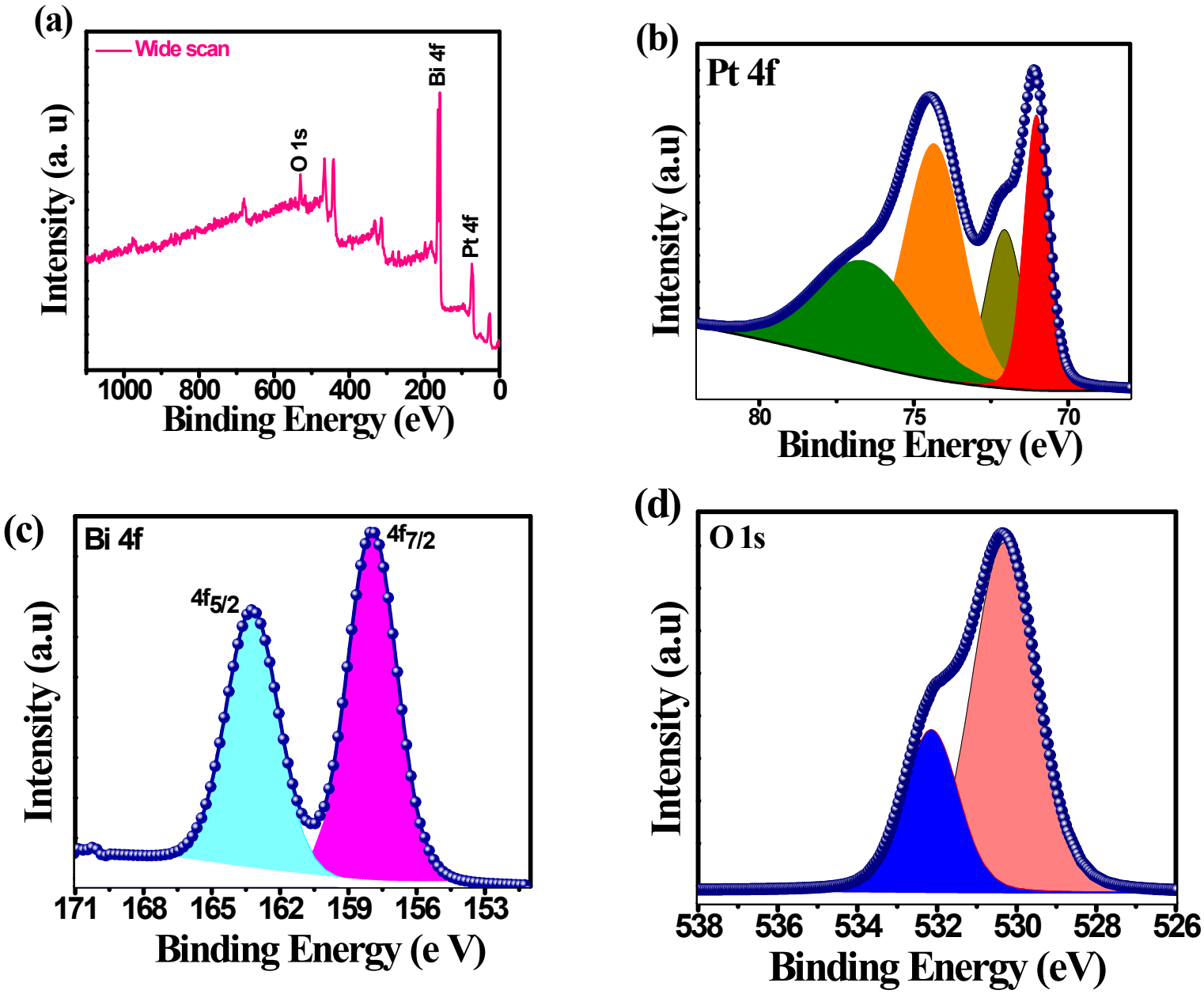

Table S2: XPS table of synthesized binary composite PB

Element	Peak	Position (B.E) eV	FWHM (eV)	Raw area (cps) ev	Atomic conc (%)
Bi 4f	$Bi4f_{7/2}$	161.25	1.70	11130.8	13.24
	$Bi4f_{5/2}$	164.67	1.72	28341.8	33.71
		159.3	1.71	36467.2	43.38
		166.54	1.63	8129.0	9.67
Pt4f	$Pt^0 4f_{7/2}$	71.03	0.945	5562.7	18.65
	$Pt^0 4f_{5/2}$	74.34	2.19	11028.3	36.98
	Pt^{2+}	72.07	1.38	4667.2	15.65
	Pt^{4+}	76.57	3.88	8563.4	28.72
O1s	O_H	530.30	1.94	4508.3	71.99
	O_L	532.14	1.63	1754.3	28.01

Table S3: XPS table of synthesized binary composite PZ

Element	Peak	Position (B.E) eV	FWHM (eV)	Raw area (cps) ev	Atomic conc (%)
Zn 2p	$Zn\ 2p_{1/2}$	1045.37	2.71	20910.3	35.80
	$Zn\ 2p_{3/2}$	1022.29	2.42	37496.6	64.20
Pt4f	$Pt^0 4f_{7/2}$	71.21	0.86	7295.9	15.23
	$Pt^0 4f_{5/2}$	74.68	1.59	13857.2	28.93
	Pt^{2+}	72.01	1.74	12099.5	25.26
	Pt^{4+}	76.35	4.39	14648.2	30.58
O1s	O_H	531.23	2.23	13190.5	68.30
	O_L	532.98	1.76	6122.5	31.70

Table S4: XPS table of synthesized ternary composite PZ25B1

Element	Peak	Position (B.E) eV	FWHM (eV)	Raw area (cps) ev	Atomic conc (%)
Bi 4f	$Bi4f_{7/2}$	157.70	2.727	252.9	51.23
	$Bi4f_{5/2}$	162.92	3.59	243.0	48.77
Zn 2p	Zn $2p_{1/2}$	1044.48	2.39	5361.5	37.06
	Zn $2p_{3/2}$	1021.4	2.11	9069.4	62.94
Pt4f	$Pt^0 4f_{7/2}$	70.33	0.87	501.9	18.36
	$Pt^0 4f_{5/2}$	73.87	1.89	1229.5	44.9
	Pt^{2+}	71.07	1.70	766.3	28.02
	Pt^{4+}	76.22	1.89	238.9	8.72
O1s	O_H	530.18	1.59	1496.90	66.74
	O_L	531.90	1.37	745.93	33.26

Fig. S4 $(\alpha h\nu)^2$ vs $h\nu$ profiles of PZ1B5, PZ1B1, PZ5B1, PZ20B1, and PZ30B1 ternary heterojunction for the determination of band gap energy.

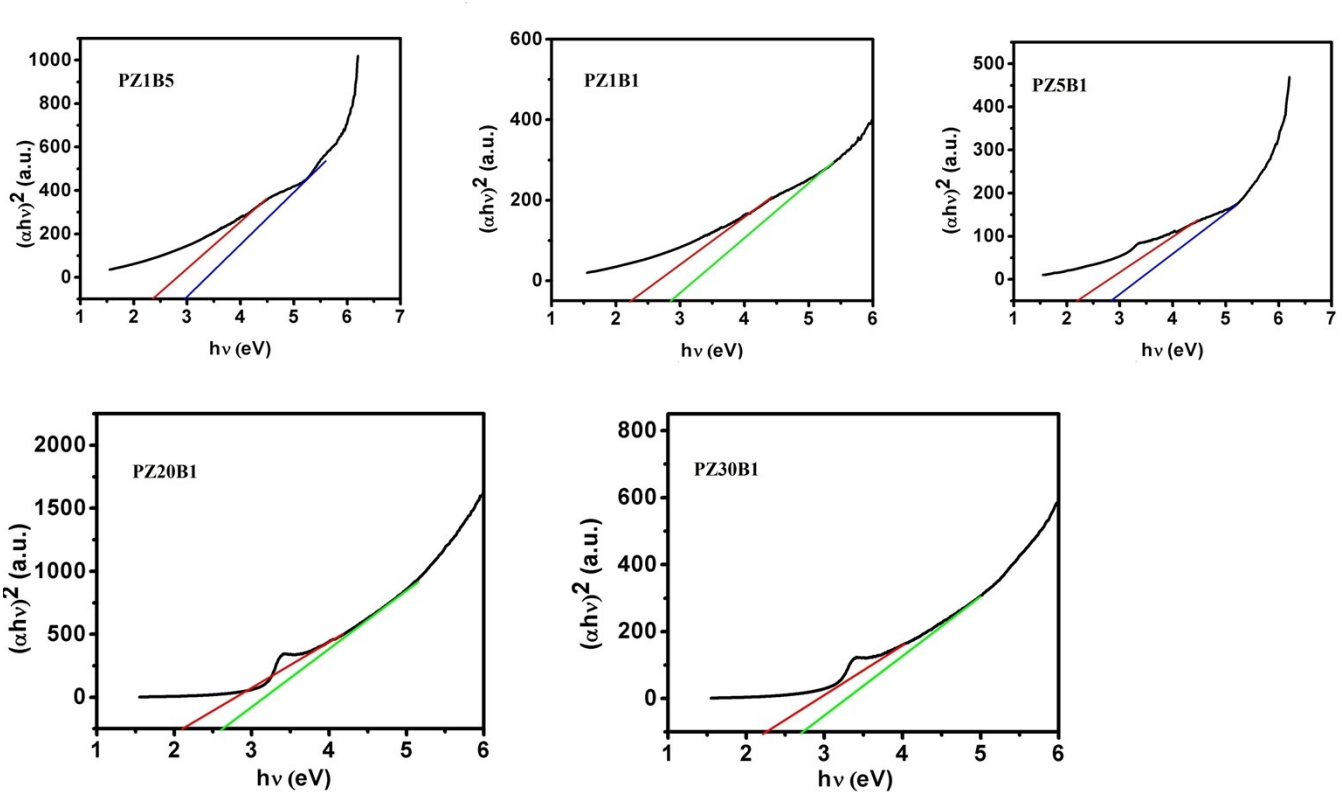

Fig. S5 Cyclic voltammograms of PZ25B1 electrode (in mA mg^{-1} of Pt) in 1 M NaOH solution in the presence and absence of visible light.

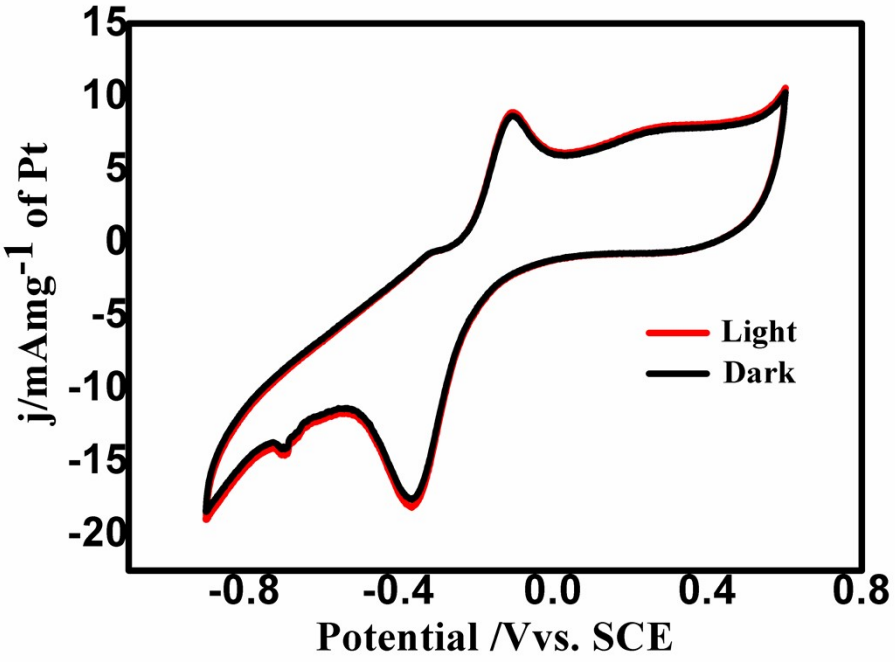

S.1 Calculation of the electrochemical active specific surface area of Pt in all synthesized catalysts

The electrochemical active specific surface area (ECSA)s of platinum in PB, PZ and different PZB composites were determined by the reduction of PtO monolayer from cyclic voltammogram (CV) of the constructed electrode immersed in 0.5 M NaOH solution, executed at scan rate 50 mVs^{-1} using the following equation:

$ECSA = Q_H / (4200 \times m)$

Where, Q_H (mC) is the charge due to the reduction of PtO as obtained fom the CVs, 4200 mC m^{-2} is the electrical charge associated with the reduction of PtO monolayer, and m is the loading of Pt metal in gram on the working electrode.

Fig. S6 Cyclic voltammograms (in $mAmg^{-1}$ of Pt) of PB, PZ, PZ1B5, PZ1B1, PZ5B1, PZ20B1 and PZ25B1 electrodes emerged in 1 M NaOH solution.

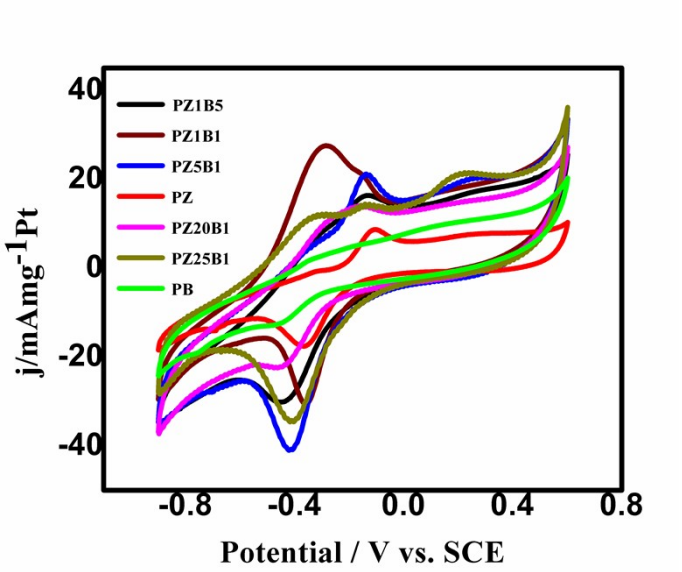

Table S5: Electrochemically active surface area of synthesized binary and ternary electrodes.

Electrode	Active surface (m^2gm^{-1})
PB	14.0
PZ	18.5
PZ1B1	20.9
PZ1B5	17.9
PZ5B1	40.5
PZ20B1	32.5
PZ25B1	30.9
PZ30B1	24.6

Table S6. Tafel slope and exchange current density data from potentiodynamic studies of electrodes based on PZ, PB, and PZB composites for methanol oxidation reaction under (A) dark and (B) light conditions at a scan rate of 1 mV s^{-1}.

A. **Dark**				B.**Light**		
Electrodes	Intercept/V	Slope/Vdec^{-1}	Exchange current density/mAmg^{-1}	Intercept/V	Slope/Vdec^{-1}	Exchange current density/mAmg^{-1}
PB	-0.461	0.081	$1.25x10^{-8}$	-0.529	0.108	$5.1x10^{-6}$
PZ	-0.540	0.129	$4.67x10^{-5}$	-0.641	0.173	$2.2x10^{-4}$
PZ1B1	-0.543	0.114	$1.34x10^{-5}$	-0.556	0.113	$1.67x10^{-5}$
PZ1B5	-0.350	0.068	$1.0x10^{-11}$	-0.518	0.080	$6.6x10^{-8}$
PZ5B1	-0.616	0.143	$4.46x10^{-4}$	-0.636	0.144	$6.4x10^{-4}$
PZ20B1	-0.608	0.090	$3.54x10^{-6}$	-0.640	0.118	$1.31x10^{-4}$
PZ25B1	-0.539	0.110	$8.31x10^{-6}$	-0.774	0.153	$4.7x10^{-3}$
PZ30B1	-0.623	0.148	$6.45x10^{-4}$	-0.720	0.147	$2.7x10^{-3}$

S2: The impact of various scan rates of the PZ25B1 electrode on the oxidation of methanol

The impact of various scan rates of the PZ25B1 electrode on the oxidation of methanol in 0.5 M CH_3OH + 1 M NaOH solution is studied and this reveals the negative shift of potential with the increase of potential scan rate (V).[50] To evaluate the transport characteristics of PZ25B1 electrode, the plot of I_p versus $V^{1/2}$ was plotted in presence and absence of light as shown in the Fig. 7d and Fig. S8 respectively. These show that the oxidation peak current is linear relationship to the square root of scan rate indicating MOR is controlled by diffusion process in both dark and light condition. The diffusion co- efficient (D_0) of the electrode is compared by equation (1) and (2).

$$I_p = (2.69 \times 10^5)\, n^{3/2} A D_0^{1/2} C_0 V^{1/2} \quad \text{.....(1)}$$

$$\frac{D_{light}}{D_{dark}} = \left[\frac{\left(\frac{i_p}{\nu^{1/2}} \right)_{light}}{\left(\frac{i_p}{\nu^{1/2}} \right)_{dark}} \right]^2 \quad \text{.....(2)}$$

Where where I_p is the anodic peak current, n is the number of electrons transferred, V is the scan rate, Co is the bulk concentration of methanol, Do is the diffusion coefficient, and A is the electrode surface area. The ratio of effective diffusion coefficients (D_{light} /D_{dark}) under two conditions is determined from Eq. 2 and the value clearly advocated that the light illumination improves the effective rate of mass transport of electro active species to the surface and around the surface of the electrode across a concentration gradient resulting in better catalytic performance.

Fig. S7 (a) CVs of PZ25B1 electrode under visible light illumination with different scan rates in 0.5 M MeOH + 1 M NaOH solution recorded at -0.3 V. (b) The plot of I_p (forward peak current density) versus $V^{1/2}$ (scan rate)$^{1/2}$ in methanol oxidation under visible light irradiation.

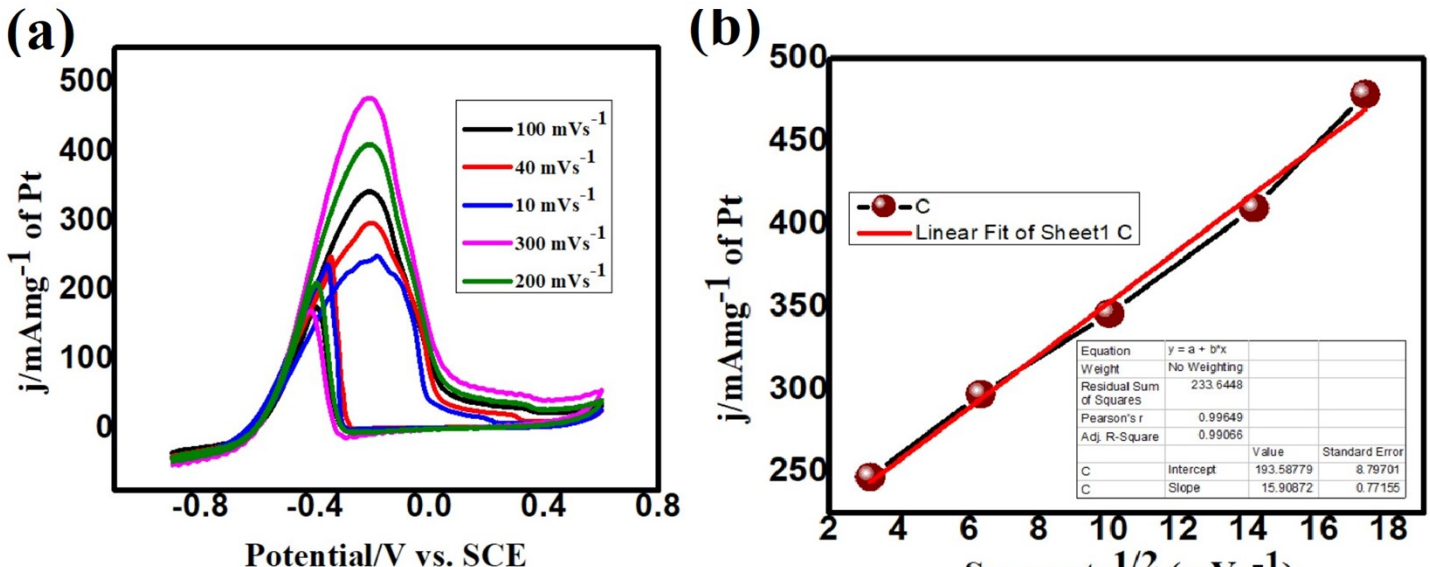

Fig. S8 CO oxidation and stripping of (a) PB (b) PZ (c) PZ25B1(d) PZ1B1(e) PZ30B1(f) PtXC72 in 0.5 M NaOH solution at a scan rate 50 mVs^{-1} and 25°C in absence of light. The solid line represents the 1st scanning cycle and the dotted line represents 2nd scanning cycle.

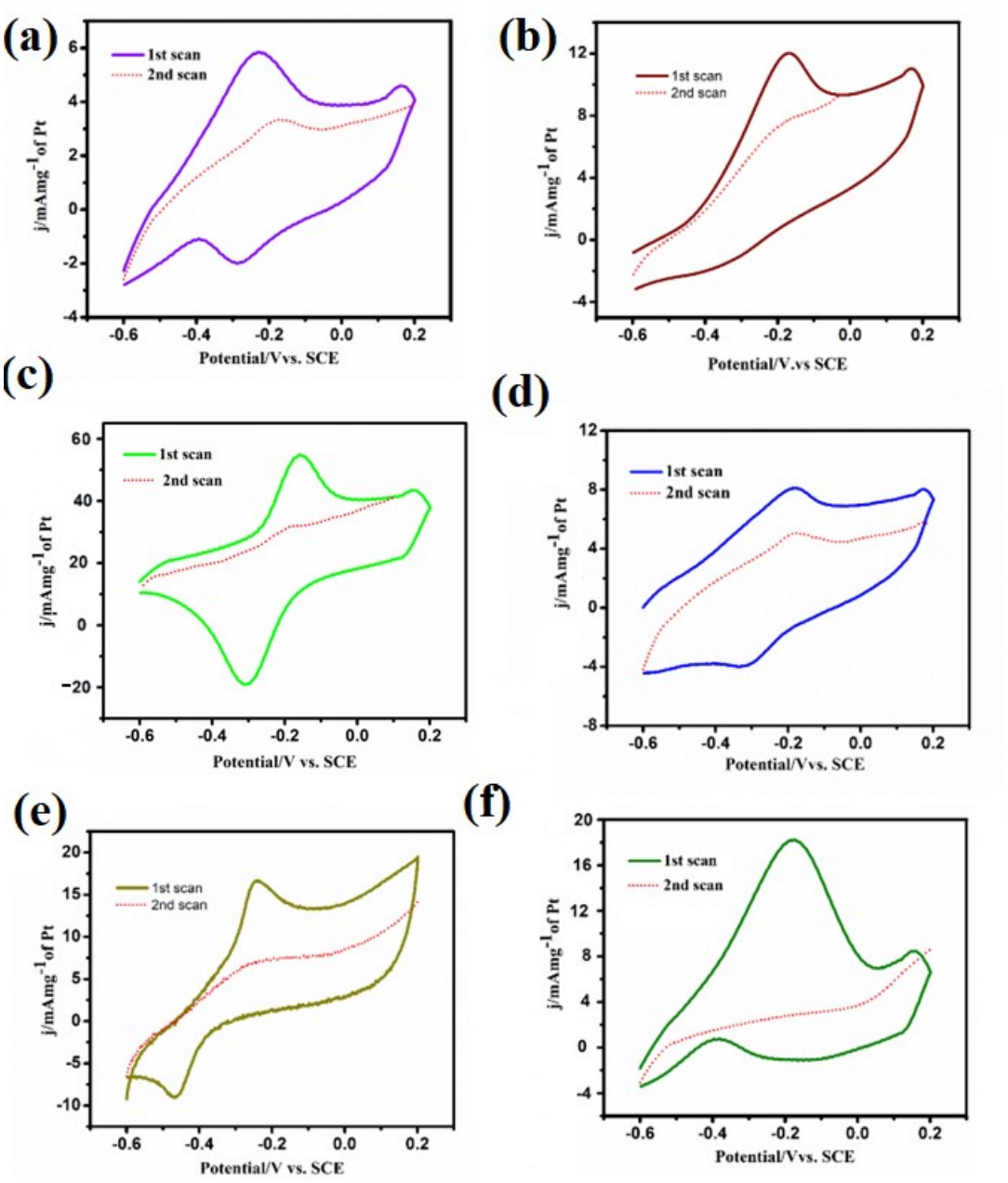

Fig. S9 The standard HPLC curves for known concentration of (a) $HCOOCH_3$ (b) HCHO (c) CO_3^{2-} (d) HCOONa (e) Oxallic acid ($C_2H_2O_4$).

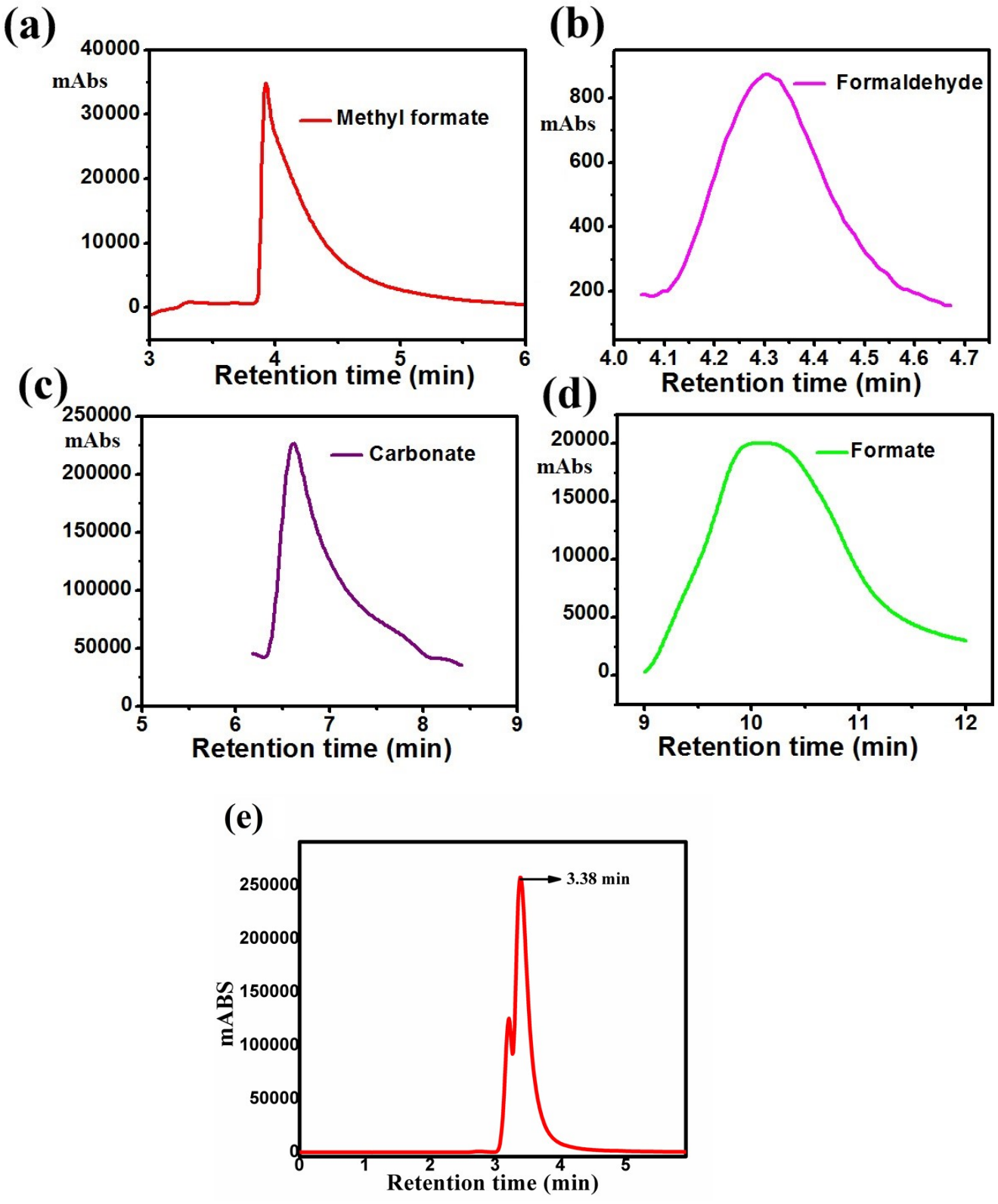

Fig. S10 The GCMS profiles of MOR products (a) PB dark (b) PB light (c) PZ dark (d) PZ light (e) PZ25B1 dark